Elucidating the ionic signals modulating the transcriptional oscillations of core circadian clock genes in Rat-1–*Per2*-luciferase fibroblasts

Jay Miguel Fonticella

NSF IRES Fellow at the Institute for Transformative Bio-Molecules

Laboratory of Animal Integrative Physiology

Nagoya University

Nagoya, Japan

ABSTRACT

Background: The mammalian circadian timing system is characterized by oscillations in the level of clock gene mRNA transcripts and encoded-proteins. While the transcriptional/translational feedback loops regulating circadian rhythms are well-known, properties such as temperature-compensated oscillations implicate ion concentrations as circadian clock modulators. In this study, the role of Na^+ and K^+ ion channels in mediating the *Per2* transcriptional oscillations of rat-1–*Per2*-luciferase fibroblasts was examined. Here, we monitored the circadian gene expression patterns in fibroblasts exposed to various ion channel inhibitors. By comparing the period length and rhythmic amplitude between chemical inhibitor groups, we seek to elucidate the ion channels modulating circadian clock maintenance. We applied real-time monitoring of gene expression rhythms and reverse transcriptase-quantitative polymerase chain reaction to quantify the inhibitory effect of protein channel blockers. **Results:** After our bioluminescence, percent amplitude, and RT-qPCR analysis, we discovered our most intriguing findings in the rat-1 fibroblasts exposed to Raxatrigine (CNV-1014802). Specifically, the Raxatrigine-treated fibroblasts demonstrated substantially attenuated mRNA cycle amplitudes and significantly atypical period lengths. Moreover, the period- and amplitude-modifying effects were also observed in the fibroblasts treated with Lansoprazole and R-lansoprazole, which were interestingly more disrupted than the previously studied KN93-treated plates. We then revealed that Lansoprazole exposure significantly decreased the hypothermic upregulation of *Per2* transcripts. **Conclusion:** While our RT-qPCR analysis could not be applied to the fibroblasts in the presence of CNV, these findings suggest a possible link between the voltage-gated NaV1.7 channel and the endogenous mechanisms mediating core circadian genes.

INTRODUCTION

Background: The mammalian circadian clock regulates a variety of biological processes, including sleep-wake cycles, body temperature, endocrine secretion, and liver metabolism patterns (Lavery et al., 1993; Portaluppi et al., 1996). With the range of physiological functions maintained by this master pacemaker, the disturbance of circadian rhythms may have detrimental health effects. Certain circadian disturbances, such as delayed sleep phase disorder, affect 0.17% of the U.S. population (The Recovery Village, 2022). Across species, the main environmental cue associated with circadian entrainment is the photoperiod. Photoperiod is the daily change in light intensity, which is perceived by the photoreceptors in the retina and circulated to the neurons of the suprachiasmatic nucleus (Takahashi, 1995; Hastings, 1997). Although the cyclic mechanisms of clock gene expression and their encoded proteins have been thoroughly described (Dunlap et al., 2017; Takahashi et al., 2017; Nohales et al., 2016), certain common properties of the circadian clock remain undefined.

The unique property of temperature-compensated oscillation is a biological function of particular interest associated with circadian rhythms (Hastings et al., 1957). While a temperature increase is known to accelerate the rates of numerous biochemical reactions, temperature-compensated oscillations signify the substantially reduced influence of temperature on the pace of the circadian clock. Although the particular proteins regulating circadian rhythms vary between species, the pathway of temperature-compensation is conserved across all circadian clock models. The investigation of the cues underpinning temperature-compensation became a focus in our laboratory, as its conservation indicated a potential mechanistic link to the machinery allowing cell-autonomous clock gene transcriptional oscillations. Moreover, by elucidating the signals driving temperature-compensation, we predicted that further insight

towards the endogenous mechanisms facilitating rhythmic clock gene expression would be gained.

Prior to the extensive studies on clock gene regulation, a feedback system consisting of ion influxes was theorized as the main molecular modulator of the circadian clock (Njus et al., 1974). Through the investigations of how the period lengths and circadian rhythms were disrupted by manipulating various ion concentrations, the membrane model was derived. This model associating ionic regulation with circadian rhythms has been recently documented in animal models. In *Drosophila*, the influxes of intracellular Ca^{2+} levels were shown to oscillate in rhythm with core circadian clock genes (Guo et al., 2016). Thus, our laboratory resolved to further investigate the regulatory role of calcium ions by targeting the Ca^{2+}/calmodulin-dependent kinase II (CaMKII) and Na^{+}/Ca^{2+} exchanger (NCX). As described in the manuscript, our laboratory concluded that targeting Ca^{2+} signaling disrupted the 3 core characteristics of the circadian clock: cell-autonomous oscillations, temperature-compensation, and entrainment (Kon and Wang et al., 2021).

These findings suggest that ionic signals mediate the maintenance of the circadian clock, including the properties of temperature-compensation and endogenous transcriptional oscillations. Currently, it remains unclear if the circadian clock in the rat-1 fibroblast model is: (1) transcriptionally regulated by other ionic signals and (2) sensitive to additional ions while undergoing the temperature-compensation response. This research aims to elucidate the underlying ion channels that regulate rat-1 fibroblast transcriptional oscillations of the *Per2* clock gene. The information gained in these experiments may provide additional insight for designing novel treatments to correct the highly prevalent circadian disruptions in our society.

EXPERIMENTAL PROCEDURES

Real-time Monitoring of Gene Expression Rhythms in Mammalian cells: To perform real-time monitoring of core circadian clock gene expression rhythms, Rat-1 fibroblasts stably expressing *Per2*-luciferase reporter were used. The cells were seeded on 35-mm dishes at a density of 1.0×10^6 cells per plate. All cells were then cultured at 37°C with 5% CO_2 in a media mainly comprised of Dulbecco's Modified Eagle's Medium (DMEM; Sigma-Aldrich #5796). The media was supplemented with 10% fetal bovine serum (FBS; Equitech-Bio Inc.) and penicillin (50U/mL). The following day, the fibroblasts were treated with 0.1 μM dexamethasone for a 2-hour period, in which the *Per2* transcriptional oscillations were synchronized. After the synchronization period, the media was replaced with a recording medium of DMEM (Air DMEM; Sigma-Aldrich #D2902) supplemented with FBS (10%), penicillin (25U/mL), and luciferin (0.1mM). The bioluminescence levels were continuously recorded in fibroblasts maintained under Air DMEM in a LumiCycle (Actimetrics).

Pharmacological Exposure: Pharmacological exposure was performed following the 2-hour incubation period with dexamethasone. These treatments included 2% DMSO (control), 5μM Raxatrigine, Lansoprazole (5μM, 10μM, and 20μM), R-lansoprazole (5μM and 10μM), KB-R7943 (5μM, 10μM, and 20μM; inhibitor standard) and KN93 (5μM and 10μM; inhibitor standard). Following this exposure period, embryos were incubated in blocker-containing Air DMEM at 37°C after loading into the LumiCycle.

Reverse Transcription Polymerase Chain Reaction Analysis: Total RNA was extracted and prepared from cultured cells using QIAzol (Qiagen) according to the manufacturer's protocol. Reverse transcription polymerase chain reaction analysis was then conducted as described previously (Kon et al., 2014).

Mathematical Analysis: To normalize and detrend plate-to-plate variation of bioluminescence counts, the raw data was first divided by the mean bioluminescence signaling calculated for 6 days. The normalized rhythms were then detrended by subtracting the 24-hour centered averages. To calculate the relative amplitude of the *Per2* expression rhythms, the area under the curve was tabulated. Similarly, period lengths were calculated using the average values of the peak-to-peak periods and trough-to-trough periods 1-day following the period of dexamethasone treatment in the rat-1 fibroblasts.

DISCUSSION

As calcium ion channels have been determined to act as molecular regulators of temperature-dependent transcriptional oscillations in multiple core circadian clock genes (Kon, N. & Wang, H.-T. et al., 2021), our laboratory predicts that additional ion channels may also serve as signals mediating properties of circadian rhythms. Ultimately, we expected to observe an association between higher concentrations of examined chemical inhibitors and abnormal clock gene expression, with Na^+ and K^+ channel blockers hypothetically resulting in the most disrupted oscillations (Table 1). Because the presence of Raxatrigine (CNV-1014802) targets a voltage-gated NaV1.7 channel, with Na^+/Ca^{2+} exchangers being implicated to modulate temperature-compensated oscillation (Kon and Wang et al., 2021), we predicted CNV exposure to most significantly disrupt circadian rhythms relative to other chemical inhibitor treatments. Because there was both a substantial attenuation in rhythm amplitude and a drastic change in period length observed in Raxatrigine-treated fibroblasts, the results support our hypothesis (Figure 6, Figure 8, Figure 9). Interestingly, these findings were consistent after exposing cells to 5 μM Raxatrigine, whereas additional ion channel blockers were tested at concentrations of 10 μM or 20 μM (Figure 8D).

Through real-time monitoring of gene expression rhythms and hypothermic gene regulation analysis, we found that fibroblasts exposed to Lansoprazole and R-lansoprazole (R-enantiomer of Lansoprazole) show atypical *Per2* transcriptional oscillations. When treated with these H^+/K^+-ATPase inhibitors, the period length and rhythmic amplitude of *Per2* transcripts significantly decreased, relative to the control group of DMSO and inhibitor standard of KN93 (Figure 6 and 9). This trend is most evident when comparing the bioluminescence counts in R-lansoprazole- and Lansoprazole-treated fibroblasts with the DMSO-treated plates (Figure 5).

We also examined the inhibitory role of Lansoprazole and R-lansoprazole exposure in temperature-compensated oscillations. The inhibitory roles of KN93 and KB-R7943 regulation in the cold tolerance signaling pathways have been thoroughly documented (Kon, N. & Wang, H.-T. et al., 2021). Specifically, these findings indicated that a temperature decrease induces an increase in clock gene expression levels, driven by the underlying mechanism of NCX-Ca^{2+}-CaMKII activity. Having observed rhythmic disruptions induced by Lansoprazole exposure similar to those induced by KN93 and KB-R7943, we then investigated whether the presence of Lansoprazole will reduce the hypothermic upregulation of *Per2* transcripts. Following a 1-day incubation at 27ºC, rat-1 fibroblasts exposed to Lansoprazole and R-lansoprazole demonstrated significantly attenuated levels of *Per2* transcripts, which were mathematically indistinguishable from levels of KN93-treated cells (Figure 11). This finding indicates that the H^+/K^+-ATPase may also act as a key protein underlying the temperature-compensation response in our model. Furthermore, the overall reduction in bioluminescence counts following H^+/K^+-ATPase inhibition supports previous membrane model manuscripts, which suggest that K^+ is a phase-shifting ion (Njus et al., 1974).

Previous work, by Kon and Wang et al., suggests that Ca^{2+} channels serve as an adaptive mechanism within rat-1 fibroblasts to mediate temperature-compensated oscillations of core circadian clock genes. Moreover, prior to studies, characterizing the regulatory underpinnings of clock genes, a feedback system modulated by ions was hypothesized as the underlying mechanism of circadian gene transcriptional oscillations (Njus et al., 1974). Taken together, the data suggests that the ion channels targeted by Raxatrigine and Lansoprazole are associated with the signaling and maintenance of *Per2* rhythmic oscillations. Determining the upstream ionic regulators of core timekeeping genes, including *Bmal1* and *Per2*, has remained as an undefined

link between circadian rhythms and the membrane model. Our studies are the first to evaluate how inhibiting the voltage-gated NaV1.7 channel and H^+/K^+-ATPase influences the expression oscillations of *Per2* transcripts in rat-1 fibroblasts. Thus, these findings recapitulate previous data regarding the role of Ca^{2+} signaling in circadian rhythms while also postulating a role for the voltage-gated NaV1.7 channel and H^+/K^+-ATPase to mediate the cell-autonomous oscillations and temperature-compensation response.

ACKNOWLEDGEMENTS

I would like to express my gratitude to Dr. Takashi Yoshimura and Dr. Naohiro Kon for welcoming me into their laboratories with guidance and mentorship. Special thanks to Dr. Hsin-Tzu Wang, Ms. Manhui Zhang, Mx. Liang Ren, and Ms. Suyi Wang for their direction and assistance throughout this project. Thank you to Dr. Junfeng Chen and all of the faculty at the Laboratory of Animal Integrative Physiology review committee for your support in evaluating my NSF IRES fellowship at the Nagoya University Institute for Transformative Bio-Molecules (ITbM).

FIGURES

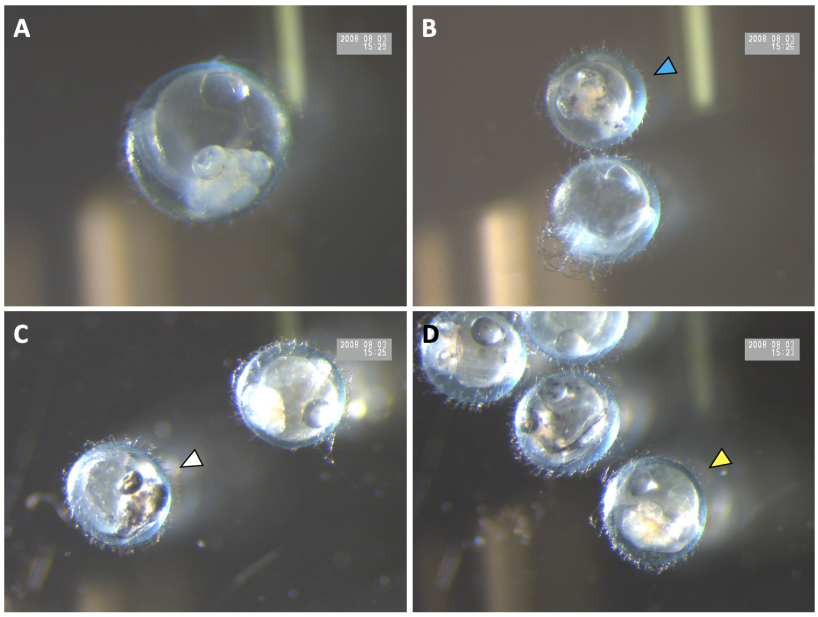

Figure 1. Representative Melanophore Phenotypes among Triple CRISPR/Cas9 Knockout Medaka embryos. Pigmentation phenotypes were recorded following triple CRISPR/Cas9 knockouts via embryonic microinjections. Representative images of medaka embryos displaying the (A) full-knockout, (B) mosaic, or (C) wild-type phenotype. Blue, white, and yellow arrowheads point to the mosaic, wildtype, and full-knockout embryos, respectively.

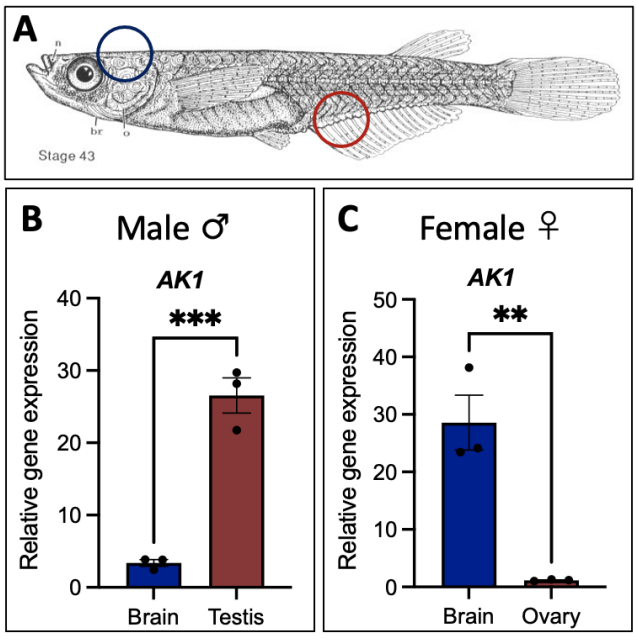

Figure 2. Reverse Transcription-quantitative Polymerase Chain Reaction on isolated tissues in adult medaka. (A) Brain and gonadal tissues were extracted from adult medaka fish,

with a corresponding schematic of extraction areas (annotated from Alonso-Barba, 2016). Relative levels of AK1 expression were compared between a (B) male and (C) female fish.

Table 1. Biological function of ion channel inhibitors used in this study

Perturbation	Biological activity	Accession Number(s)
Lansoprazole	Neutral sphingomyelinase inhibitor	DB11706 (DrugBank)
Raxatrigine	Voltage-gated sodium channel (Nav1.7) blocker	DB00448 (DrugBank)
R-lansoprazole	Proton pump and H^+/K^+-ATPase inhibitor	DB05351 (DrugBank)
KN93	Ca^{2+}/calmodulin-dependent kinase II inhibitor	ab120980 (Abcam)
KB-R7943	Na^+/Ca^{2+} exchange inhibitor	ab120284 (Abcam)

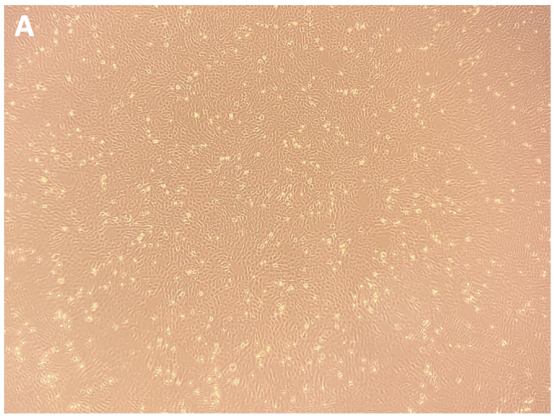

Figure 3. Parameters of targeting ion channels associated with circadian rhythms. A set of channel blockers disrupting rhythmic circadian gene expression were used. (A) Representative image of rat-1 fibroblasts in which transcriptional oscillations were examined further.

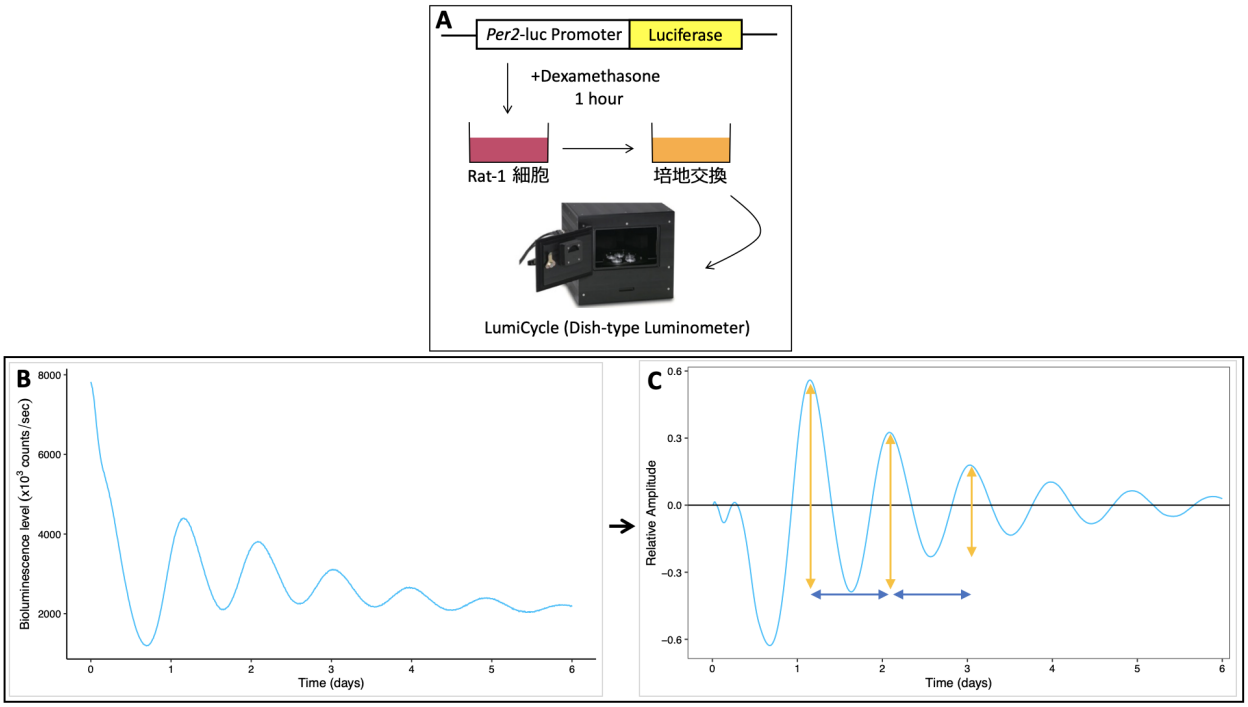

Figure 4. Experimental setup for Rat-1–*Per2*-luciferase fibroblast data collection. (A) Rat-1 fibroblasts stably expressing *Per2*-luciferase reporter were cultured. Following a 1-hour incubation in dexamethasone wherein transcriptional rhythms synchronized, cells were plated in inhibitor-containing media. These 35-mm cell culture dishes were then loaded into the LumiCycle. (B) Using a previously published mathematical model, carried out by Kim et al., the

recorded bioluminescence counts were normalized and detrended to further analyze (C) relative rhythmic changes, including amplitude (orange) and period (blue) parameters.

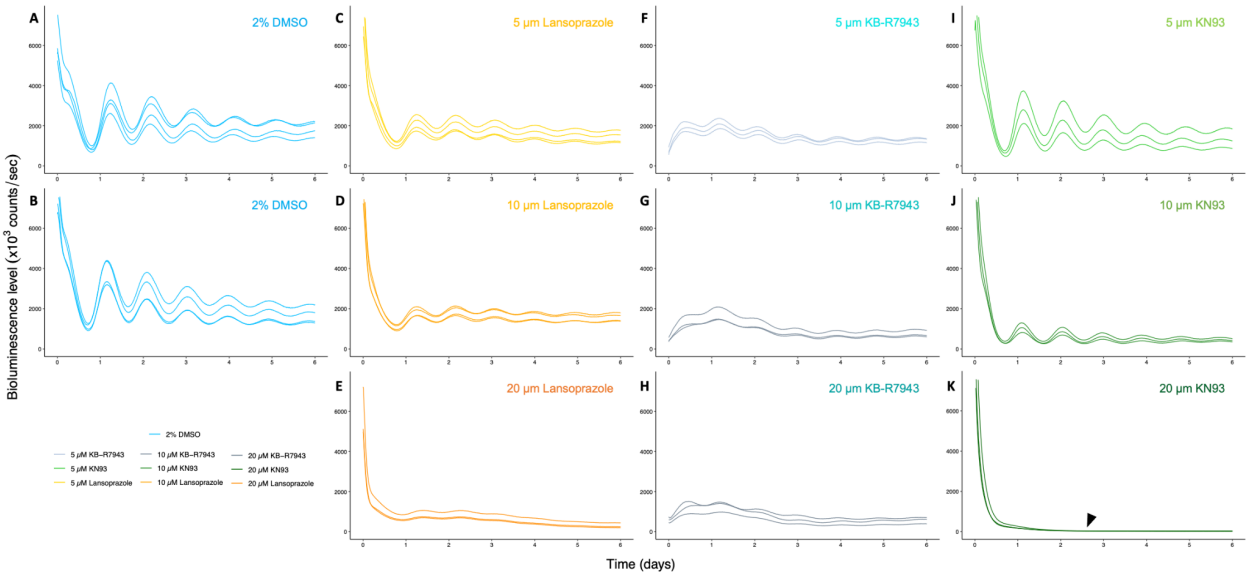

Figure 5. Difference in Bioluminescence Counts between Lansoprazole-, KB-R7943-, and KN93-treated rat-1 fibroblasts. Representative bioluminescence levels were shown for fibroblasts maintained in (A,B) 2% DMSO, Lansoprazole at (C) 5 μM (D) 10 μM and (E) 20 μM, KB-R7943 at (F) 5 μM (G) 10 μM and (H) 20 μM, and KN93 at (I) 5 μM (J) 10 μM and (K) 20 μM. The black arrowhead indicates cell death in the respective plate. N = 2 independent samples, n = 3-4 plates in each chemical inhibitor group per sample.

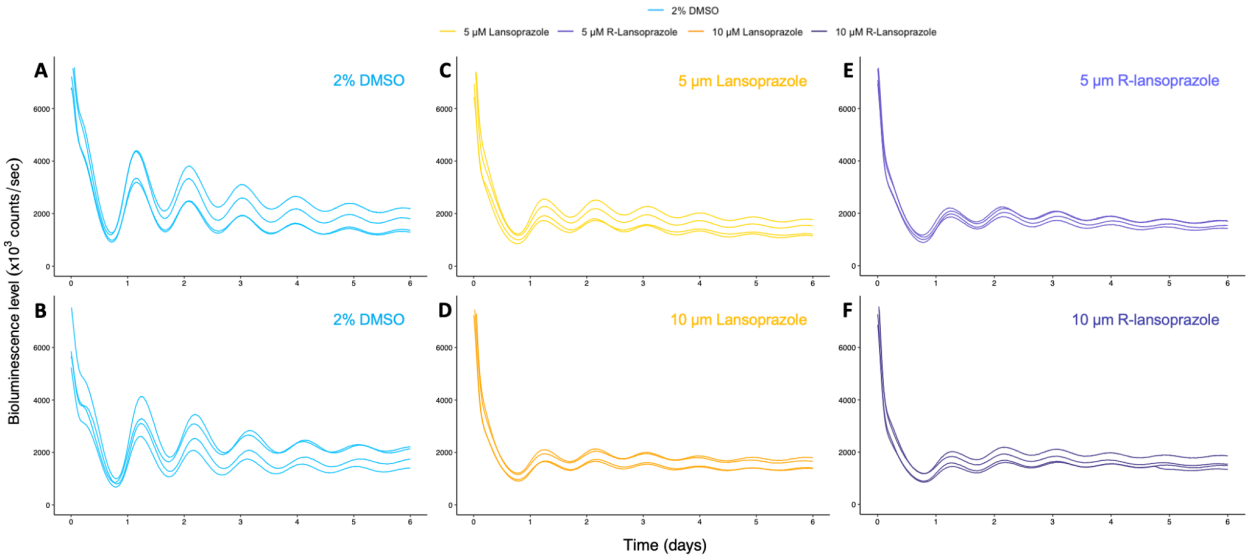

Figure 5. Comparison of Bioluminescence Counts between Lansoprazole- and Dexlansoprazole-treated rat-1 fibroblasts. Representative bioluminescence levels were shown

for fibroblasts maintained in (A,B) 2% DMSO, Lansoprazole at (C) 5 µM and (D) 10 µM, and R-lansoprazole at (E) 5 µM and (F) 10 µM. N = 2 independent samples, n = 3-4 plates in each chemical inhibitor group per sample.

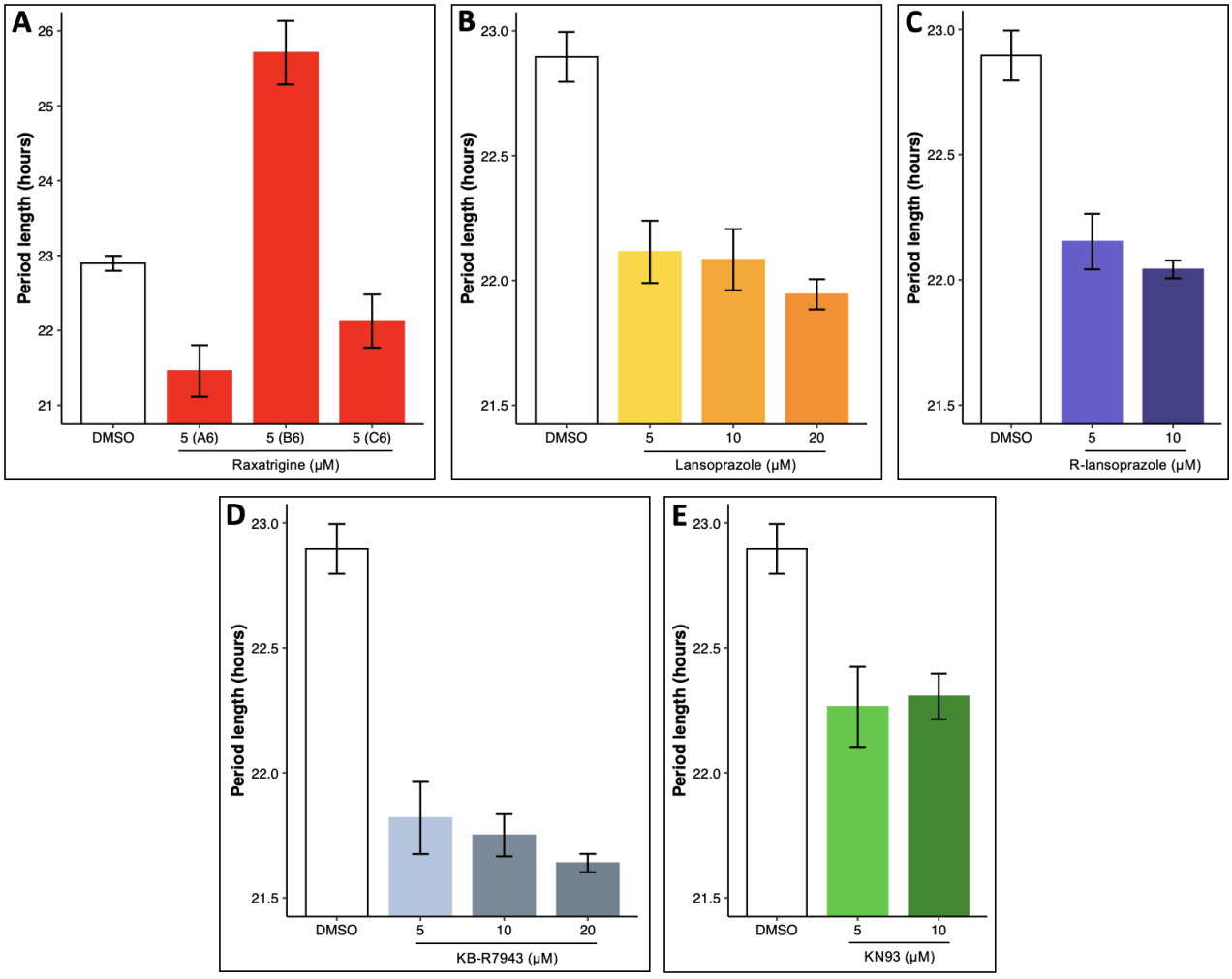

Figure 6. Period length changes of Rat-1–*Per2*-luciferase cells in the presence of chemical inhibitors. Representative period shortening and lengthening effects of (A) Raxatrigine at 5 µM, (B) Lansoprazole at 5 µM, 10 µM, and 20 µM, (C) R-lansoprazole at 5 µM, 10 µM, and 20 µM, (D) KB-R7943 at 5 µM, 10 µM, and 20 µM, and (E) KN93 at 5 µM and 10 µM, setting the 2% DMSO-treated plates as the control group. N = 2 independent samples, n = 3-4 plates in each ion channel inhibitor group per sample.

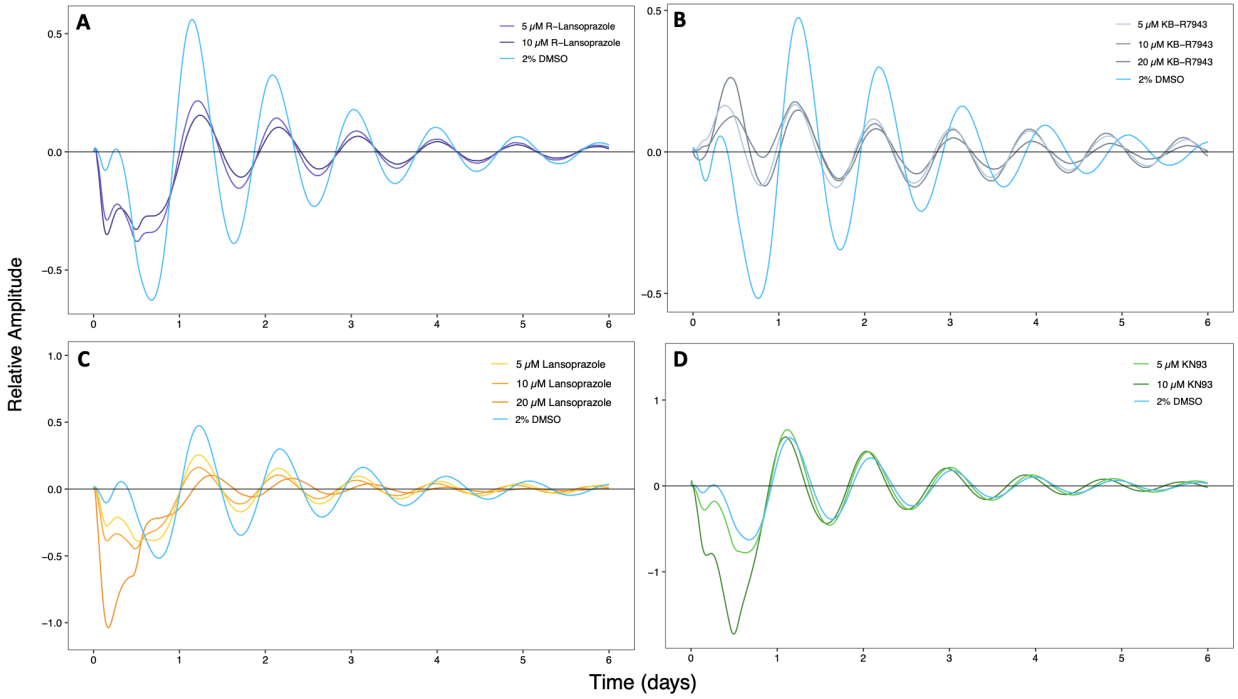

Figure 7. Representative relative rhythms of Rat-1–*Per2*-luc cells in the presence of varying concentrations of R-lansoprazole, KB-R7943, Lansoprazole, and KN93. The normalized and detrended amplitudes are shown for (A) R-lansoprazole, (B) KB-R7943, (C) Lansoprazole, and (D) KN93 at the respective concentrations, relative to the DMSO-treated control group.

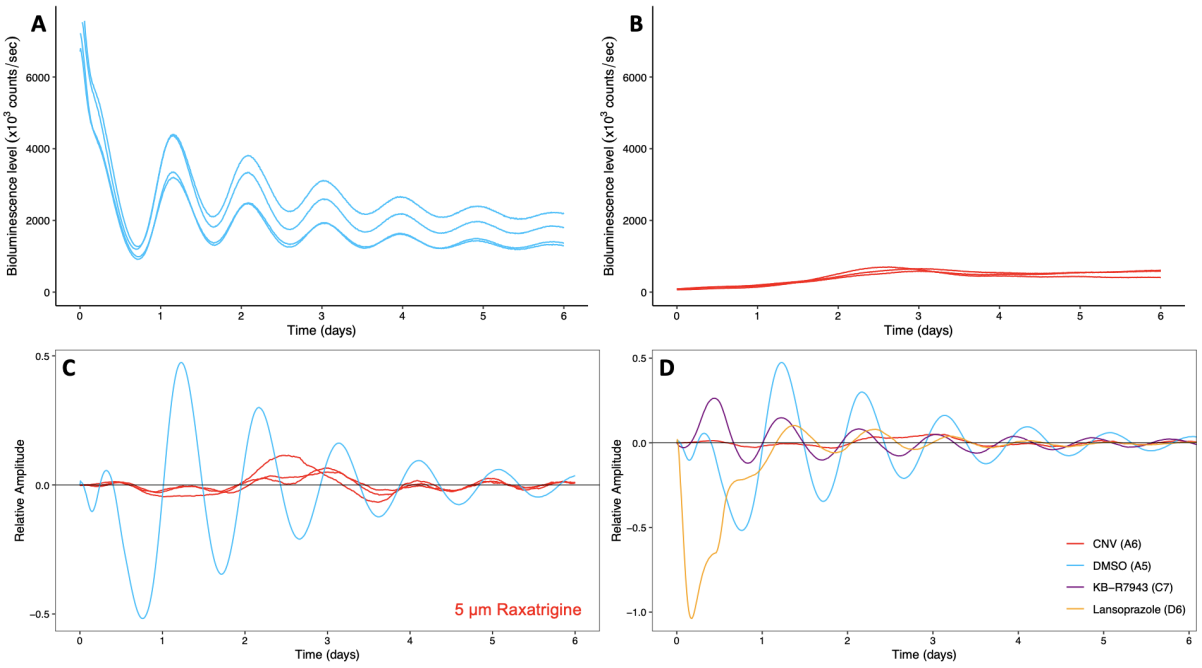

Figure 8. Disruptive effect of Raxatrigine presence on bioluminescence counts and relative rhythms in Rat-1–*Per2*-luc cells. The bioluminescence levels were shown in samples treated

with (A) 2% DMSO and (B) 5 µM Raxatrigine. The relative amplitude was plotted in samples treated with (C) 5 µM Raxatrigine and (D) across Lansoprazole-, KB-R7943-, and Raxatrigine-treated plates, relative to the DMSO-treated sample.

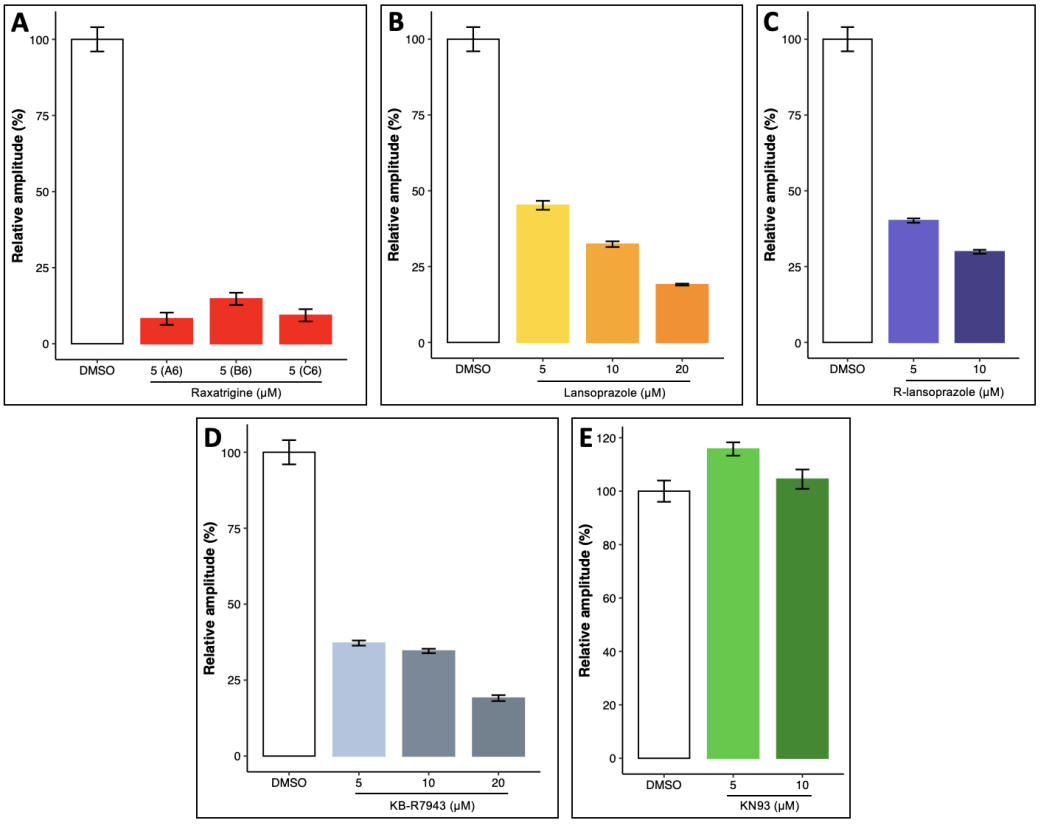

Figure 9. Relative amplitude changes of Rat-1–*Per2*-luciferase cells in the presence of chemical inhibitors. Representative amplitude decreased or increasing effects of (A) Raxatrigine at 5 µM, (B) Lansoprazole at 5 µM, 10 µM, and 20 µM, (C) R-lansoprazole at 5 µM, 10 µM, and 20 µM, (D) KB-R7943 at 5 µM, 10 µM, and 20 µM, and (E) KN93 at 5 µM and 10 µM, relative to the 2% DMSO-treated control group.

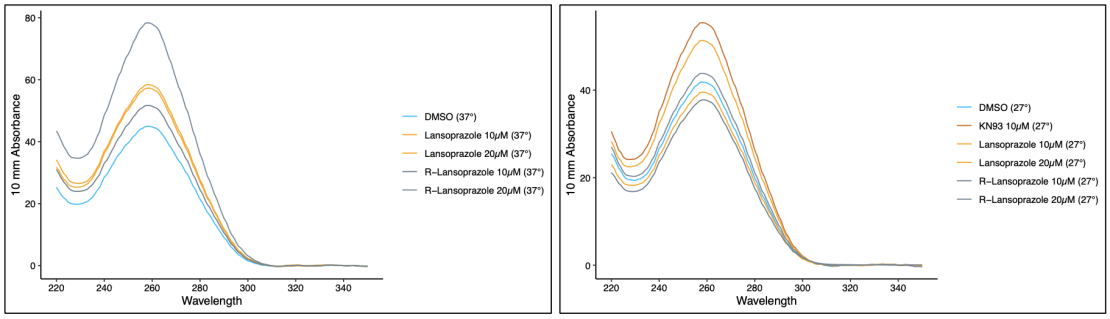

Figure 10. 260/280 Ratio of Absorbance across Rat-1–*Per2*-luciferase fibroblasts. Representative data from NanoDrop RNA quantification analysis at 37°C (left) and 27°C (right).

The 260/280 curve was assessed across each chemical inhibitor group following incubation at the higher and lower temperature.

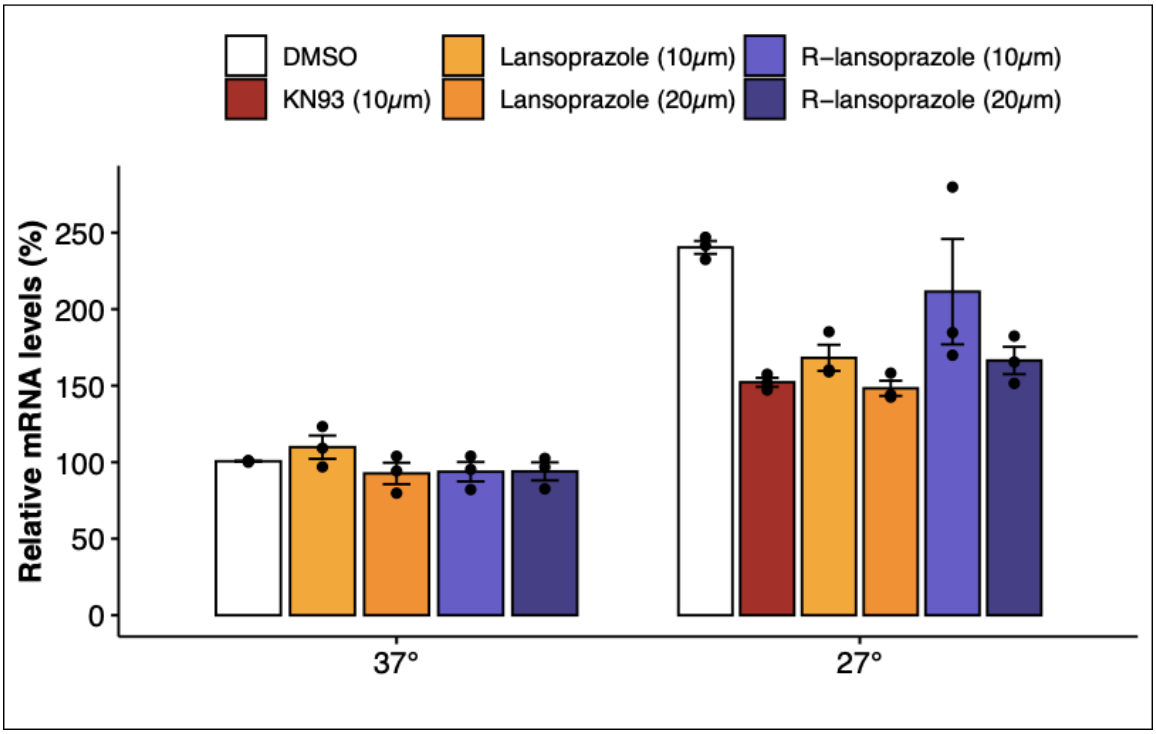

Figure 11. Lansoprazole and R-lansoprazole modulate the hypothermic-dependent upregulation of Per2 mRNA levels in Rat-1 fibroblasts. Representative data from Reverse Transcription-quantitative Polymerase Chain Reaction experiment among cells treated with chemical inhibitors at 37ºC (left) and 27ºC (right).

References

Alonso-Barba, J., Rahman, R.-U., Wittbrodt, J., Mateo, J. (2016). MEPD: medaka expression pattern database, genes and more. *Nucleic Acids Research* **44**, 819-821.

Balsalobre, A., Damiola, F., Schibler, U. (1998). A Serum Shock Induces Circadian Gene Expression in Mammalian Tissue Culture Cells. *Cell* **93**, 929-937.

Dunlap, J.C., Loros, J.J. (2017). Making time: Conservation of biological clocks from fungi to animals. *Microbiology Spectrum* **5**, 3.

Guo, F., Yu, J., Jung, H.J., Abruzzi, K.C., Luo, W., Griffith, L.C., Rosbash, M. (2016). Circadian neuron feedback controls the Drosophila sleep-activity profile. *Nature* **536**, 292–297.

Hastings, M.H. (1997). Circadian clocks. *Current Biology* **7**, 670-672.

Hastings, J.W., Sweeney, B.M. (1957). On the mechanism of temperature independence in a biological clock. *Proc. Natl. Acad. Sci. U.S.A.* **43**, 804–811.

Kon, N., Wang, H.-T., Kato, Y.S., Uemoto, K., Kawamoto, N., Kawasaki, K., Enoki, R., Kurosawa, G., Nakane, T., Sugiyama, Y., Tagashira, H., Endo, M., Iwasaki, H., Iwamoto, T., Kume, K., Fukada, Y. (2021). Na+/Ca2+ exchanger mediates cold Ca2+ signaling conserved for temperature-compensated circadian rhythms. Science Advances 7, eabe8132.

Kon, N., Yoshikawa, T., Honma, S., Yamagata, Y., Yoshitane, H., Shimizu, K., Sugiyama, Y., Hara, C., Kameshita, I., Honma, K.I., Fukada, Y. (2014). CaMKII is essential for the cellular clock and coupling between morning and evening behavioral rhythms. *Genes & Development* 28, 1101–1110.

Lavery, D.J., Schibler, U. (1993). Circadian transcription of the cholesterol 7α hydroxylase gene may involve the liver-enriched bZIP protein DBP. *Genes & Development* **7**, 1871-1884.

Nagoshi, E., Saini, C., Bauer, C., Laroche, T., Naef, F., Schibler, U. (2004). Circadian Gene Expression in Individual Fibroblasts: Cell-Autonomous and Self-Sustained Oscillators Pass Time to Daughter Cells. *Cell* **119**, 693-705.

Njus, D., Sulzman, F.M., Hastings, J.W. (1974). Membrane model for the circadian clock. *Nature* **248**, 116-120.

Nohales, M.A., Kay, S.A. (2016). Molecular mechanisms at the core of the plant circadian oscillator. *Nature Structural & Molecular Biology* **23**, 1061–1069.

Portaluppi, F., Vergnani, L., Manfredini, R., Fersini, C. (1996). Endocrine mechanisms of blood pressure rhythms. *Annals of the New York Academy of Sciences* **783**, 113-131.

Takahashi, J.S. (1995). Molecular neurobiology and genetics of circadian rhythms in mammals *Annual Review of Neuroscience* **18**, 531-553.

Takahashi, J.S. (2017). Transcriptional architecture of the mammalian circadian clock. *Nature Reviews Genetics* **18**, 164–179.

The Recovery Village Drug and Alcohol Rehab. (2022). Circadian Rhythm Sleep-Wake Disorders Statistics. *Umatilla, FL*.

Ueda, H., Chen, W., Adachi, A. (2002). A transcription factor response element for gene expression during circadian night. *Nature* **418**, 534-539.